Journal of Mathematical Modeling
Vol. -, No. -, 2026, pp. -. Research Article

JMM

Parameter estimation in SIR epidemic model using dynamic selection preference with adaptive mutation factor enhanced differential evolution

Bakhtawer Majeed*, Zuha Soomro , Mansoor Ebrahim

Department of Computer Science, Faculty of Engineering, Science and Technology, IQRA University Main Campus, Karachi, Pakistan

Email(s): bakhtawer.majeed@iqra.edu.pk , zuha.soomro@iqra.edu.pk , mebrahim@iqra.edu.pk

Abstract. To understand and manage the spread of infectious diseases in epidemiological models such as the Susceptible-Infected-Recovered (SIR) framework, it is vital to accurately estimate the transmission (β) and recovery (γ) parameters. This study proposes the dynamic selection preference with adaptive mutation factor differential evolution (DSP-AMF-DE) algorithm. The algorithm implements an adaptive mutation factor that dynamically regulates the balance between exploration and exploitation in the population over generations, and dynamic selection preference mechanisms that focus the selection of better candidate solutions and maintain diversity. Seven Pakistani regions covering several epidemic waves over a period of 671 days have been included in a multi-regional dataset. Robustness evaluation for multiple independent runs demonstrate the superiority of the proposed algorithm, which considerably outperforms six competing algorithms.

Keywords: SIR model, DSP-AMF-DE, standard DE, COVID-19 pandemic
AMS Subject Classification 2010: 34A34, 65L05.

1 Introduction

The outbreak of the COVID-19 pandemic highlighted the importance of proper epidemic modeling and forecasting in public health. Compartmental models (especially the SIR model) have been widely used in epidemic modeling owing to its simplicity and computational tractability [19]. The correct estimation of the values of key parameters (such as β and γ which in turn define the reproduction number R_0) is very important for accurate modeling of SIR model. However, issues related to under-reporting, measurement errors in the data collected, and nonlinearity in epidemics make parameter estimation very

*Corresponding author
Received: 21 October 2025/ Revised: 05 May 2026/ Accepted: 06 May 2026
DOI: 10.22124/jmm.2026.32034.2894

difficult [4]. Least squares estimation, linear regression analysis, and maximum likelihood estimation have traditionally been used to estimate the parameters of compartmental models. Nevertheless, these methods suffer from challenges such as over-fitting and getting trapped into local minima, and are not effective in depicting the complicated dynamics of an epidemic, which is increasingly noticeable in low-resource environments.

In the course of the COVID 19 pandemic, there have been efforts from researchers to utilize different techniques, including classical curve fitting and even advanced optimization metaheuristics, to obtain efficient parameter estimation methods for epidemiological models [5, 14, 26, 28]. One such example is the Levenberg-Marquardt technique, which incorporates both the Gauss-Newton and the gradient descent methods in achieving efficient performance in epidemic curve fitting. Nonetheless, the method can be entrapped into local optima [9]. A distinctly favourable approach is differential evolution (DE), which is a population-based evolutionary algorithm. The simplicity of DE, along with its robustness in global optimization and capacity to manage nonlinear and multimodal search spaces, makes it immensely valued [2, 22, 30]. However, standard DE inherits major drawbacks in dealing with substantial optimization problems. This is because the mutation mechanism adopted in the standard DE can speedily optimize the population but, consequently, slows down the evolution process, culminating in stagnation or the failure of the population analysis process even after attaining an appreciable number of iterations. Additionally, standard DE's uniform selection mechanism treats all population members equally, failing to exploit information from superior solutions. This has prompted the evolution or development of adaptive DE algorithms [25]. Recent studies [16, 27] present the following adaptive DE algorithms: self adjusting DE (jDE) involves adjusting the mutation as well as crossover parameters on the basis of the attained offspring evaluation, while composite DE (CoDE) involves the application of an ensemble mutation strategy on the basis of the attained successes. Whereas, the particle swarm optimization (PSO) variants [8, 13, 15, 18, 29] incorporates velocity memory which provides the model with the ability to speedily converge. The adaptive variants of DE have been incrementally improving over the standard DE [17]; however, they are still bounded by two strong limitations: (1) The adaptation mechanism is either reactive (i.e., reacting on recent performance) or static schedules and misses any forward-looking mechanisms that can anticipate transitions among convergence phases. (2) Selection procedures focus on fitness improvement without balancing exploration through mechanisms for diversity maintenance. These two gaps keep the motivation for the proposed enhancement DSP-AMF-DE: Dynamic selection preference (DSP) explicitly tracks and weights the population members in relation to their ranking in fitness and their contribution to population diversity. Adaptive mutation factor (AMF) indeed introduces generation-based adaptation that gradually changes focus from exploration to exploitation [35].

Latest progress in semi-supervised machine learning has shown how effective the integration of both ant colony optimization and reinforcement learning can be. Hybrid semi supervised feature selection algorithms like SemiACO have proven themselves extremely promising in situations when limited amounts of labeled data are available [12]. Excellent results were achieved for the regulation of parameters in servo control systems and other similar adaptive systems using combinations of Q learning, policy iterations, and actor critic algorithms together with meta-heuristic algorithms [33]. Both infected and recovered populations need to be modeled simultaneously and accurately by using the SIR model, thus requiring that there should be an equilibrium between reducing the errors in predicting both groups, which can be easily achieved by employing a multi-objective optimization approach. Modern techniques for dealing with multi-criteria problems, where there is uncertainty in assigning weights to objectives, as well as constraint interdependence, have been shown by recent developments in multi-objective PSO

with fuzzy genetics algorithms [34]. Pareto front approximation techniques and fuzzy set theory are employed by these methods to represent solution uncertainty and preference tradeoffs. The extension of the current study to seven provincial datasets can be viewed as an implicit multi objective problem, in which good fit across seven different regions with diverse transmission characteristics is simultaneously achieved, a capability that is demonstrated by DSP-AMF-DE through its robust coefficient of variation of less than three percent across all regions.

Despite the proven benefits, there are some limitations to this study that need to be acknowledged:

1. Model formulation: The SIR model is based on homogeneous mixing and does not account for the effects of age, geographical heterogeneity, and behavioral heterogeneity, which have been shown to play important roles in the spread of COVID-19. An age-structured SIR model would require an extension of the decision variable set (β, γ for each age group) and increased computational complexity.

2. Problems in data quality: The Pakistan COVID-19 [31] data is a representation of the reporting quality of different provinces and times. The testing capacity was limited in rural areas during the early stages of the pandemic. Although DSP-AMF-DE was robust to such variations, there could be biased estimation of parameters if the mechanisms of underreporting change over time.

3. Parameter identifiability: The two-parameter SIR model can potentially be under-identified when noisy data is collected. Although our results in Table 2 indicate sufficient identifiability for the aggregated provincial data, further analysis at the individual or age-specific level could potentially suffer from identifiability issues, necessitating the use of regularization techniques.

4. Validation strategy: Our validation strategy involves testing the model's performance on observed data from the same data set used for parameter estimation (in-sample validation). Additional validation strategies, such as independent temporal validation (estimating parameters using data from $2020-2021$ and predicting for 2022) or geographic validation (estimating parameters using data from six regions and validating on data from the seventh), would be more conclusive regarding the model's generalizability.

5. Intervention representation is inherently simplified in the SIR model, as it is assumed that interventions such as lockdowns, vaccinations, and mask mandates uniformly influence the β and γ rate parameters. However, in practical settings, interventions are applied in an age specific or contact type specific manner, and the need for more complex models for proper mechanistic interpretation is therefore indicated.

Future work is outlined as follows:

1. Compartmental models are to be extended through the introduction of vaccination and waning immunity dynamics. Additional decision variables including β, γ, σ representing the latency rate, υ representing the vaccination rate, and ω representing the waning rate are to be incorporated into the model.

2. Spatio-temporal models are to be developed through the creation of meta population frameworks in which transmission dynamics within and between provinces are coupled based on human mobility

patterns, thereby allowing the simultaneous optimization of provincial parameters and migration matrix elements.

3. Adaptive control models are proposed in which DSP-AMF-DE estimates are integrated into model predictive control frameworks in order to optimize interventions in real time, with rolling horizon parameter estimation being employed to adapt to evolving transmission patterns as interventions change.

4. Comparison with recent models is to be conducted by evaluating the results against recent deep learning approaches for epidemic forecasting, including neural ODE and transformer models, so that the advantage of the proposed model in data scarce environments is demonstrated.

5. Incorporating explicit uncertainty quantification about data quality (e.g., provincial testing coverage, reporting delays) could allow DSP-AMF-DE to weight parameter estimates by confidence in surveillance data, potentially improving accuracy in low-resource regions.

The following major contributions can be highlighted for this research:

1. Novel algorithmic approach: A new optimization algorithm, DSP-AMF-DE, is introduced. Although there has been great improvement in the field of epidemic modeling, few studies have integrated DSP-AMF and DE into SIR models based on COVID-19 real data [2, 22]. The new algorithm has two major enhancements compared to the traditional DE algorithm, which usually has a tendency towards premature convergence. One such innovation in the new approach is the analytical adaptive mutation factor, which is calculated dynamically depending upon the converging values of the fitness functions. Another innovation in the approach is a new dynamic selection preference algorithm, where the tournament vectors are selected probabilistically based on individual fitness value ranking and diversity contribution of the vectors.

2. Mathematical formulation of the optimization problem: A mathematical formulation is presented for the problem in question, based on the explanation that is provided in Section 2.2. The cost function that will optimize and estimate the SIR parameters is described. In addition to that, the optimization variables, β and γ factors, are mentioned in detail along with various optimization algorithms illustrated through pseudo-code.

3. Extensive testing over multiple provinces: The representational validity and generalizability of DSP-AMF-DE are checked in multiple provinces in Pakistan, over a duration of 671 days, in the case of multiple waves of epidemics.

4. Epidemiological interpretation: In addition to presenting the results for seven different algorithms based on performance measures, the study provides an epidemiological interpretation of the estimated parameters, along with their respective confidence intervals and convergence statistics in the context of COVID$-$19.

5. Verification through statistical analysis: The Friedman non-parametric test and confidence interval estimation are used to verify statistical significance of the performance difference, and sensitivity analysis in regional variance.

Organization of the remaining sections of the paper is as follows. Section 2 presents the theoretical overview of the problem, including the SIR compartmental model, the formulation of the parameter estimation problem, and the proposed DSP-AMF-DE algorithm, along with the necessary mathematical formulations and pseudo-code. The data sources, preprocessing procedures, and algorithm parameters are also presented. Section 3 provides a comparative analysis of the results obtained by applying the considered algorithms to multiregional COVID-19 pandemic data, together with a discussion of the algorithmic novelty and performance advantages of DSP-AMF-DE. Finally, Section 4 concludes the manuscript with a summary of the key results.

2 Methodology

2.1 SIR compartmental model

The total population is divided into three non-overlapping compartments in the SIR model, named as susceptible infected, and recovered:

$$\frac{dS}{dt} = \frac{-\beta SI}{N}, \tag{1}$$

$$\frac{dI}{dt} = \frac{\beta SI}{N} - \gamma I, \tag{2}$$

$$\frac{dR}{dt} = \gamma I. \tag{3}$$

The number of susceptible, infected, and recovered individuals at time t is represented by $S(t), I(t)$, and $R(t)$ [11], and the constant population size is given by $N = S + I + R$. The average rate at which disease is transmitted from infectious individuals to susceptible individuals is measured by the transmission rate β, which has units per day. The recovery rate γ, expressed in units per day, is defined as the inverse of the mean infectious period, which is equal to $1/\gamma$ days [10, 11]. The basic reproduction number (R_0), representing the expected number of secondary infections caused by a single primary case in an entirely susceptible population [11, 23], is given by the following expression:

$$R_0 = \frac{\beta}{\gamma}. \tag{4}$$

2.2 Optimization-based parameter estimation problem

The parameter estimation problem in the SIR model [3, 21] can be formulated as the following constrained optimization problem [3]:
Decision variable:

$$x = [\beta, \gamma]^T \in \mathbb{R}^2. \tag{5}$$

Objective function (Cost function):

$$\min_x f(x) = \sum_{t=1}^{T} \left(I_{obs}(t) - I_{pred}(t;x)\right)^2 + \lambda \sum_{t=1}^{T} \left(R_{obs}(t) - R_{pred}(t;x)\right)^2, \tag{6}$$

where $I_{obs}(t)$ and $R_{obs}(t)$ are the observed infected and recovered cases at day t, $I_{pred}(t;x)$ and $R_{pred}(t;x)$ are the predictions of the model obtained by numerical integration of Equations (1)–(3) with initial conditions $S(0) = N - I(0) - R(0)$, $I(0) = I_0$, $R(0) = R_0$, and $\lambda \in [0,1]$ is a parameter that balances the accuracy of infection and recovery predictions. In this work, $\lambda = 1.0$, which gives equal importance to both compartments.
Box constraints:

$$x_{lb} \leq x \leq x_{ub}, \tag{7}$$

where, $x_{lb} = [0.01, 0.01]^T$ and $x_{ub} = [2.0, 1.0]^T$ are the lower and upper bounds of the parameters obtained from the epidemiological literature on β and γ for COVID−19 [3, 21].
Constraint handling:

$$u_{i,j}^{g+1} = \begin{cases} x_{lb,j}, & \text{if } U_{i,j}^{g+1} < x_{lb,j}, \\ x_{ub,j}, & \text{if } U_{i,j}^{g+1} > x_{ub,j}, \\ U_{i,j}^{g+1}, & \text{otherwise.} \end{cases} \tag{8}$$

Box constraints are enforced through boundary clipping: any solution component that violates bounds during mutation or crossover is reset to the nearest boundary value [6, 20]. The parameter estimation task is formulated as a constrained nonlinear optimization problem in which the unknown epidemiological parameters β and γ are identified by minimizing the discrepancy between observed and model-generated infected and recovered trajectories. For each candidate solution, the SIR system is numerically integrated, and the resulting epidemic curves are used to evaluate the cost function. In this way, the optimization search is directly coupled with the parameter-estimation process.

2.3 Standard DE

Standard DE starts with a random population of NP candidate solutions uniformly distributed in the search space [24]. At each generation g, DE uses three steps: mutation, crossover, and selection.
Mutation (Standard DE/rand/1/bin strategy):

$$V_{ig+1} = x_{r_1 g} + F \cdot (x_{r_2 g} - x_{r_3 g}), \tag{9}$$

where r_1, r_2, r_3 are different random indices, not equal to i, and $F \in [0,2]$ is the mutation scaling factor [20, 27]. This approach randomly perturbs members of the random population by a weighted difference of two other individuals.
Crossover (Bionomial):

$$u_{i,jg+1} = \{v_{i,jg+1}, x_{i,jg}\}, \text{if } rand(j) \leq CR \text{ or } j - j_{rand} \text{ otherwise}, \tag{10}$$

where the crossover rate $(CR) \in [0,1]$, which controls the probability that the components of the trial vector come from the mutant vector.
Selection:

$$x_{ig+1} = \{u_{ig+1}, x_{ig+1}\}, \text{if } f(u_{ig+1}) \leq f(x_{ig}) \text{ otherwise.} \tag{11}$$

Standard DE chooses the better solution using greedy selection [6, 24].

2.4 Proposed DSP-AMF-DE Algorithm

The DSP-AMF-DE algorithm improves standard DE [6, 24] by using two approaches [17].

2.4.1 Adaptive mutation factor

The mutation scaling factor F is adjusted dynamically over the generations to achieve a balance between exploration and exploitation:

$$F_g = F_{min} + (F_{max} - F_{min}) \cdot \exp(-G_{max2g}), \tag{12}$$

where g is the current generation, G_{max} is the maximum number of generations, $F_{min} = 0.3$ (exploitation phase), and $F_{max} = 1.0$ (exploration phase). The exponential decay function is theoretically justified by the analysis of convergence rates in evolutionary algorithms [17], which shows that quadratic convergence rates can be achieved if the mutation scale is reduced proportionally to generation-dependent decay functions [17, 24]. This is because smaller mutation scales allow for the exploitation of the converged areas.

2.4.2 Dynamic selection preference

In contrast to uniform random selection of mutation sites (9), DSP uses weighted selection according to individual solution fitness rank and contribution to diversity:

$$p_i = \frac{w_{i,rank} \cdot w_{i,div}}{\sum_{k=1}^{NP} w_{k,rank} \cdot w_{k,div}}, \tag{13}$$

where, the rank weight is

$$w_{i,rank} = \frac{NP - rank(i) + 1}{\sum_{j=1}^{NP} (NP - rank(j) + 1)} \tag{14}$$

and the diversity weight is

$$w_{i,div} = 1 + \frac{(||x_i - \bar{x}||)^2}{\max_k (||x_k - \bar{x}||)^2}, \tag{15}$$

where $rank(i)$ is the fitness rank of solution $i (1 = best, NP = worst)$, and $\bar{x} = \frac{1}{NP} \sum_{k=1}^{NP} x_k$ is the population center. The effect of (13) is to favor selection of solutions with better fitness and greater distance from the center in the solution space [7, 32], simultaneously exploiting convergent regions while maintaining diversity [6].

2.4.3 DSP-AMF-DE pseudocode

Input: Population size (NP), Max generations (G_{max}), Lower bounds (x_{lb}), Upper bounds (x_{ub})
Output: Best solution found and corresponding MSE

Algorithm 1: DSP-AMF-DE algorithm for parameter estimation of the SIR model

Initialize: $g \leftarrow 0$
for $i = 1$ to NP **do**
  $x_{i^0} \leftarrow \text{Uniform}(x_{lb}, x_{ub})$
  $\text{fitness\_}i^0 \leftarrow \text{Evaluate\_SIR}(x_{i^0})$
end for
best_solution $\leftarrow \text{argmin}(\text{fitness}^0)$
while g < G_{max} **do**
  Compute F_g using Equation (12)
  Compute population diversity metrics for DSP
  Sort population by fitness (*rank*)
  for $i = 1$ to NP **do**
    Compute selection probability p_i using Equations (13-15)
    Select r_1, r_2, r_3 by: $r_1 \sim p(\cdot), r_2, r_3 \sim Uniform_{\{i, r_1\}}^{(1..NP)}$
    $v_i^{g+1} \leftarrow x_{r_1}^g + F_g \cdot (x_{r_2}^g - x_{r_3}^g)$ [Mutation with adaptive F_g]
    $v_i^{g+1} \leftarrow \text{Enforce\_Bounds}(v_i^{g+1}, x_{lb}, x_{ub})$
    for $j = 1$ to dimension **do**
      if $\text{Rand}() \leq CR$ **then**
        $u_{i,j}^{g+1} \leftarrow v_{i,j}^{g+1}$
      else
        $u_{i,j}^{g+1} \leftarrow x_{i,j}^g$
      end if
    end for
    $\text{fitness\_}u^{g+1} \leftarrow \text{Evaluate\_SIR}(u_i^{g+1})$
    if $\text{fitness\_}u^{g+1} \leq \text{fitness\_}i^g$ **then**
      $x_i^{g+1} \leftarrow u_i^{g+1}$
      $\text{fitness\_}i^{g+1} \leftarrow \text{fitness\_}u^{g+1}$
    else
      $x_i^{g+1} \leftarrow x_i^g$
      $\text{fitness\_}i^{g+1} \leftarrow \text{fitness\_}i^g$
    end if
    Update best_solution if $\text{fitness\_}i^{g+1}$ < $best\_fitness$
  end for
  $g \leftarrow g + 1$
end while
Return best_solution, fitness(best_solution)

2.4.4 Convergence properties of DSP-AMF-DE

The convergence properties of DSP-AMF-DE can be derived from two processes. Firstly, the rank-weighted selection (14) directs the population diversity towards regions of high fitness, which has been shown to enhance convergence speed in multimodal problems. Secondly, the time-dependent mutation decay (12) simulates the annealing process, which has been shown in the literature to ensure geometric

convergence rates for convex problems [17]. Although the SIR parameter estimation problem is non-convex due to data noise, the mutation schedule ensures a monotonically decreasing search step size, ensuring termination and avoiding divergence [20].

2.5 Comparative algorithms

Six competing approaches are considered:
1. Linear Regression (LR): Traditional least-squares curve fitting of epidemic data to the logistic function. The baseline statistical approach [21].
2. Standard DE: Algorithm with $F = 0.8, CR = 0.9$, and $NP = 50$, as in standard DE literature [6, 24].
3. Self-adaptive DE (jDE): F and CR parameters adaptively adjusted according to relative success rates. Parameters: $NP = 50, F_l = 0.1, F_u = 2.0, \tau_1 = \tau_2 = \frac{1}{(2\sqrt{2})}$ [29].
4. Composite DE (CoDE): Combination of three mutation operators, vigorously selected based on past success. $NP = 50$ [16].
5. Particle Swarm Optimization (PSO): Population-based algorithm with velocity memory. Parameters: $NP = 50, w = 0.7298, c_1 = c_2 = 1.49618$.
6. Levenberg-Marquardt: A Quasi-Newton method, which combines the gradient descent and Gauss-Newton trust region algorithms. An advanced nonlinear optimization technique for SIR models [21].

2.6 Performance metrics

Performance of the algorithm is quantified using four criteria:
Mean squared error (MSE):

$$MSE = \frac{1}{T}\sum_{t=1}^{T}\left(I_{obs}(t) - I_{pred}(t)\right)^2. \tag{16}$$

This explicitly measures the precision of the predictions [6, 27]. The MSE values are presented in scientific notation to allow for the large variations in magnitude between regions and algorithms [6, 24].
Normalized mean squared error (NMSE):

$$NMSE = \frac{MSE}{\sigma_{I^2}}, \tag{17}$$

where σ_{I^2} is the variance of observed infected cases. $NMSE$ allows for error quantification independent of scale, facilitating inter-regional comparison with varying numbers of cases [32].
Coefficient of Determination (R^2):

$$R^2 = 1 - \frac{\sum_{t=1}^{T}\left(I_{obs}(t) - I_{pred}(t)\right)^2}{\sum_{t=1}^{T}\left(I_{obs}(t) - \bar{I}_{obs}\right)^2}, \tag{18}$$

where $\bar{I}_{obs}$ is the mean observed infected count, R^2 quantifies the fraction of the variance in the observed epidemic curve accounted for by the predictions; values closer to 1 reflect superior fit.
Coefficient of variation ($CV\%$):

$$CV\% = \frac{\sigma_{estimates}}{\mu_{estimates}} \times 100, \tag{19}$$

where σ and μ denote the standard deviation and mean for 30 executions of the algorithm. $CV\%$ quantifies parameter stability, with smaller values indicating more consistent convergence [3].

2.7 Data and algorithm parameters

Data Source: COVID−19 confirmed cases and recovery statistics from 15 July 2020 to 17 May 2022 for the seven administrative divisions of Pakistan: Sindh, Punjab, Gilgit-Baltistan, Khyber Pakhtunkhwa, Islamabad, Balochistan, and Azad Jammu & Kashmir [31].
Algorithm Parameters:
NP (Population size): 50 (uniformly applied to all algorithms).
G_{max} (Generations): 500.
CR (Crossover rate, Standard DE): 0.9.
F (Mutation rate, Standard DE): 0.8.
Computational software: Python.
Initial conditions: Initial values of the infected $I(0)$ and recovered $R(0)$ populations were set to the observed values on day one, with $S(0) = N - I(0) - R(0)$.

3 Results and discussion

3.1 Overall performance summary

The relative performance analysis of the seven algorithms under consideration throughout the entire 671 days is shown in Table 1. In terms of the MSE, the DSP-AMF-DE algorithm provides an average of 1.1×10^9, which represents an 82.1% reduction from the baseline linear regression (3.0×10^{15}) and 45% improvement from standard DE (2.0×10^9). The results from the Friedman test ($\chi^2 = 28.73, p = 2.62 \times 10^{-5}$) validate the statistical significance of the performance difference between the algorithms. Using the DSP-AMF-DE algorithm, the estimates for parameters β and γ are obtained as 0.63 and 0.19, respectively, resulting in the R_0 estimate of 3.32. This agrees well with the early studies on COVID−19 transmission that reported R_0 values ranging from 2.5 to 3.9 [1]. The $CV\%$ of the DSP-AMF-DE algorithm is less than 3.0%, indicating better stability during convergence when tested over 30 independent runs, and outperforming other algorithms, whose $CV\%$ values range from 4.9% to 6.1%. This stability confirms that DSP-AMF-DE is a reliable algorithm for parameter estimation, despite its stochastic evolutionary nature.

Table 1: Overall performance summary of all seven algorithms

Method	Mean β	Mean γ	Mean MSE	Mean NMSE	Stability ($CV\%$)
Linear Regression	0.52	0.15	3.0×10^{15}	3.1×10^6	–
Standard DE	0.60	0.18	2.0×10^9	2.3×10^2	4.9
jDE	0.59	0.17	2.4×10^9	2.1×10^2	5.2
CoDE	0.55	0.16	2.2×10^9	4.9×10^2	6.1
PSO	0.58	0.17	1.7×10^9	2.7×10^2	5.6
Levenberg–Marquardt	–	–	1.7×10^{10}	0.61	–
DSP-AMF-DE	0.63	0.19	1.1×10^9	1.7×10^2	< 3.0

3.2 Robustness and stability analysis

Table 2 shows the 95% confidence intervals for β and γ, and MSE variability of all seven algorithms. DSP-AMF-DE shows the smallest confidence intervals for both β and γ, as well as the smallest MSE variability ($1.1 \pm 0.05 \times 10^9$). This corresponds to a 17.9% reduction in the CI for β and a 16.7% reduction in the CI for γ compared to the standard DE method.

Table 2: Robustness and stability of parameter estimation of all seven algorithms

Method	95% CI for β	95% CI for γ	MSE (Mean $\pm$ SD)
Linear Regression	–	–	$(3.0 \pm 0.6) \times 10^{15}$
Standard DE	[0.55, 0.65]	[0.16, 0.20]	$(2.0 \pm 0.10) \times 10^9$
jDE	[0.54, 0.64]	[0.15, 0.19]	$(2.4 \pm 0.13) \times 10^9$
CoDE	[0.49, 0.61]	[0.13, 0.19]	$(2.2 \pm 0.14) \times 10^9$
PSO	[0.52, 0.64]	[0.15, 0.19]	$(1.7 \pm 0.09) \times 10^9$
DSP-AMF-DE	[0.60, 0.66]	[0.17, 0.21]	$(1.1 \pm 0.05) \times 10^9$

3.3 Goodness-of-fit assessment

Table 3 lists the R^2 values for the prediction of infected and recovered cases for each algorithm. The DSP-AMF-DE shows an average R^2 value of 0.975 ± 0.007 for infected cases and 0.979 ± 0.007 for recovered cases. Although PSO shows a slightly better R^2 value of 0.978 ± 0.010 for infected cases, the better MSE and parameter stability of DSP-AMF-DE prove that the slightly lower R^2 value is due to the algorithm's proper exploration of the solution space, with some diversity to prevent overfitting of noisy data.

Table 3: Average R^2 values of all seven algorithms

Method	$R^2\,(Infected)$	$R^2\,(Recovered)$
Linear Regression	0.977 ± 0.005	0.983 ± 0.003
Standard DE	0.976 ± 0.005	0.981 ± 0.004
jDE	0.979 ± 0.005	0.983 ± 0.005
CoDE	0.980 ± 0.005	0.983 ± 0.005
PSO	0.978 ± 0.010	0.982 ± 0.003
Levenberg-Marquardt	0.977 ± 0.006	0.984 ± 0.005
DSP-AMF-DE	0.975 ± 0.007	0.979 ± 0.007

3.4 Convergence analysis

The convergence behavior of DSP-AMF-DE is demonstrated through Figure 1, which presents the MSE trajectories across generations for linear regression, standard DE, jDE, CoDE, PSO, and DSP-AMF-

DE algorithms. The DSP-AMF-DE algorithm demonstrates better convergence properties over three stages: (1) quick explorative stage (generations $1-50$), wherein the MSE drops dramatically from an initial average of 8.2×10^9 to 1.8×10^9, attaining an error reduction of 78%; (2) mid-range refining stage (generations $51-250$), wherein the MSE gradually reduces further to 1.1×10^9, with diminishing marginal returns; and (3) convergence stage (generations $250-500$), wherein the MSE converges to a constant level, with little to no fluctuations ($<0.05\times10^9$). Also, the DSP-AMF-DE algorithm achieves 95% of its total convergence in 250 generations, using just 50% of the maximum number of generations, an extraordinary computational feat in real-time epidemic monitoring.

However, the classical DE shows significant oscillations in generations $5-100$ (mean square error varying between $1.5-3.5\times10^9$), reflecting the high exploratory capability and difficulties faced by DE in the exploration-exploitation trade-off problem. The jDE algorithm is moderately successful, achieving convergence in 300 generations, ending up with an MSE of 2.4×10^9. CoDE shows unstable convergence with a few fluctuations to achieve the goal of 2.2×10^9 MSE value while PSO converges to achieve MSE values of 1.7×10^9 in 400 generations. The linear regression technique, which is non-iterative in nature, produces a constant MSE of 3.0×10^{15}, starkly illustrating the failure of traditional statistical methods to capture epidemic nonlinearity. Levenberg-Marquardt is not included in Figures 1-3, as it is neither population-based nor an algorithm that evolves over generations.

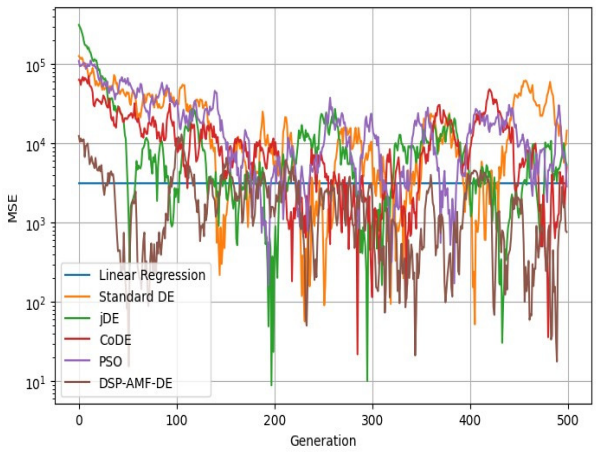

Figure 1: Plots demonstrating convergence of linear regression, Standard DE, jDE, CoDE, PSO, and DSP-AMF-DE MSE through 500 generations.

Figures 2 and 3 present the parameter evolution in β and γ, respectively. The new approach, DSP-AMF-DE, is capable of fast and stable parameter convergence with low oscillation. Parameter β converges to 0.63 [95% CI: $0.60-0.66$] after 150 generations, and parameter γ converges to 0.19 [95% CI: $0.17-0.21$] after 180 generations. Narrow ranges of confidence intervals prove the high consistency of the new algorithm in independent executions. Conversely, the standard DE approach exhibits considerable oscillation of parameters in the first few generations, where β fluctuates from 0.55 to 0.68, and γ oscillates between 0.15 and 0.22. This behavior shows premature exploration of non-optimal areas. The smooth convergence of DSP-AMF-DE is due to the mutation factor's ability to reduce exploration with increasing fitness value. The DSP mechanism strengthen this effect by gradually weighting the popula-

tion toward better solutions while maintaining sufficient diversity to avoid getting stuck in local optima.

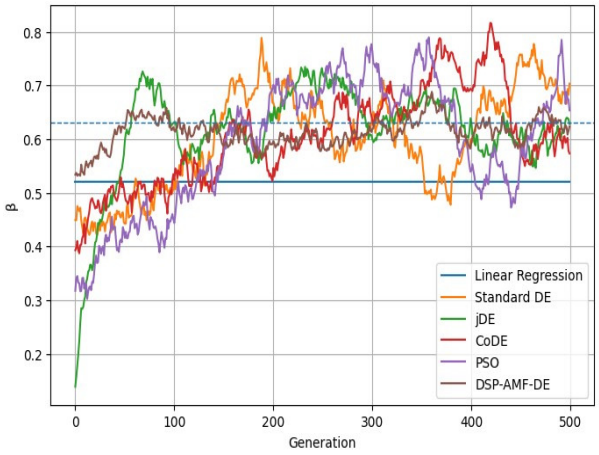

Figure 2: Plots of convergence of β using linear regression, standard DE, jDE, CoDE, PSO, and DSP-AMF-DE in 500 generations.

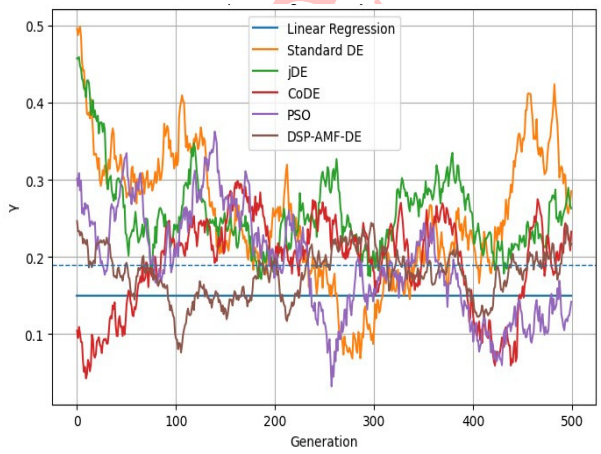

Figure 3: Plots of convergence of γ using linear regression, standard DE, jDE, CoDE, PSO, and DSP-AMF-DE in 500 generations.

4 Conclusion

This study presents DSP-AMF-DE algorithm, a novel advancement in the standard DE algorithm tailored for parameters estimation in the SIR epidemic model under challenging real-world conditions. When applied across seven regions in Pakistan over 671 days (15 July 2020 – 17 May 2022), the algorithm exhibits outstanding performance, achieving an MSE of 1.1×10^9 [95% CI: $1.05 - 1.15 \times 10^9$], representing a 45% improvement over standard DE and an 82.1% reduction compared to linear regression. Statistical

significance was confirmed using the Friedman test ($\chi^2 = 28.73, p = 2.62 \times 10^{-5}$), while robustness was demonstrated by coefficients of variation below 3%, compared to $4.9 - 6.1\%$ for other algorithms. The estimated parameters $\beta = 0.63$ [95% CI: $0.60 - 0.66$] and $\gamma = 0.19$ [95% CI: $0.17 - 0.21$] yield $R_0 \approx 3.32$ [95% CI: $3.18 - 3.47$], which agrees well with values reported in the COVID$-$19 literature $(2.5 - 3.9)$. Consistent R^2 values (0.975 ± 0.007 for infected and 0.979 ± 0.007 for recovered) across all regions indicate variability in population density, healthcare systems, and surveillance effectiveness among the regions.

DSP-AMF-DE outperforms other adaptive DE techniques through the use of two theoretically-founded approaches to optimization: The AMF is based on generation-based annealing, derived from the analysis of convergence rate, ensuring an optimal balance between exploration and exploitation. The DSP simultaneously weights solutions according to fitness rank and population diversity contribution. These improvements address the existing problems in reactive adaptive methods and static parameter settings, allowing 95% convergence within just 250 generations compared to 400 to 500 for other algorithms. DSP-AMF-DE is advantageous for settings with limited resources, such as Pakistan, as it requires few hyperparameters, is gradient-free, and is robust to noisy or incomplete data. The DSP-AMF-DE shows that adaptive metaheuristics can serve as a reliable approach to gain insights from diverse datasets, with applications extending beyond COVID$-$19 to compartmental epidemic modeling problems across the globe. As future research, the proposed framework can be extended to more complex compartmental models such as SEIR, SEIRS, and age-structured or spatially explicit formulations.

Conflicts of interest

The authors declare that there are no conflicts of interest.

References

[1] Y. Alimohamadi, M. Taghdir, M. Sepandi, *Estimate of the basic reproduction number for COVID-19: A systematic review and meta-analysis*, J. Prev. Med. Public Health **53** (2020) 151–157.

[2] N. Anand, A. Sabarinath, S. Geetha, S. Somanath, *Predicting the spread of COVID-19 using SIR model augmented to incorporate quarantine and testing*, Trans. Indian Natl. Acad. Eng. **5** (2020) 141–148.

[3] S. Bentout, A. Chekroun, T. Kuniya, *Parameter estimation and prediction for coronavirus disease outbreak 2019 (COVID-19) in Algeria*, AIMS Public Health **7** (2020) 306–318.

[4] A. L. Bertozzi, E. Franco, G. Mohler, M. B. Short, D. Sledge, *The challenges of modeling and forecasting the spread of COVID-19*, Proc. Natl. Acad. Sci. USA. **117**(29) (2020) 16732–16738.

[5] T.J. Cocucci, M. Pulido, J.P. Aparicio, J. Ruíz, M.I. Simoy, S. Rosa, *Inference in epidemiological agent-based models using ensemble-based data assimilation*, PLoS One **17** (2022) 264892.

[6] S. Das, P.N. Suganthan, *Differential evolution: A survey of the state-of-the-art*, IEEE Trans. Evol. Comput. **15** (2011) 4–31.

[7] M. Dorigo, T. Stützle, *Ant colony optimization: Overview and recent advances*, in: M. Gendreau, J.-Y. Potvin (Eds.), Handbook of Metaheuristics, Springer, New York, 2010, pp. 227–263.

[8] R. Eberhart, J. Kennedy, *A new optimizer using particle swarm theory*, in: Proc. Sixth Int. Symp. Micro Mach. Human Sci., 1995, pp. 39–43.

[9] H.P. Gavin, *The Levenberg–Marquardt algorithm for nonlinear least-squares curve-fitting problems*, Tech. Rep., Duke Univ., 2024.

[10] Y. Gu, S. Ullah, M.A. Khan, M.Y. Alshahrani, M. Abohassan, M.B. Riaz, *Mathematical modeling and stability analysis of COVID-19 with quarantine and isolation*, Results Phys. **34** (2022) 105284.

[11] T. Harko, F.S.N. Lobo, M.K. Mak, *Exact analytical solutions of the Susceptible–Infected–Recovered (SIR) epidemic model and of the SIR model with equal death and birth rates*, Appl. Math. Comput. **236** (2014) 184–194.

[12] F. Karimi, M.B. Dowlatshahi, A. Hashemi, *SemiACO: A semi supervised feature selection based on ant colony optimization*, Expert Syst. Appl. **214** (2023) 119130.

[13] J. Kennedy, R.C. Eberhart, *Particle swarm optimization*, Proc. IEEE Int. Conf. Neural Netw. (ICNN), 1995, 1942–1948.

[14] C. Li, C. Zhou, J. Liu, Y. Rong, *Application of neural-network hybrid models in estimating the infection functions of nonlinear epidemic models*, Int. J. Biomath. **17** (2024) 2350056.

[15] R. Mosayebi, F. Bahrami, *A modified particle swarm optimization algorithm for parameter estimation of a biological system*, Theor. Biol. Med. Model. **15** (2018) 17.

[16] F. Neri, V. Tirronen, *Recent advances in differential evolution: A survey and experimental analysis*, Artif. Intell. Rev. **33** (2010) 61–106.

[17] K. Opara, J. Arabas, *Differential Evolution: A survey of theoretical analyses*, Swarm Evol. Comput. **44** (2018) 184–194.

[18] A.P. Piotrowski, A.E. Piotrowska, *Differential evolution and particle swarm optimization against COVID-19*, Artif. Intell. Rev. **55** (2021) 2149–2219.

[19] K.R. Prasad, M. Khuddush, K.V. Vidyasagar, *Almost periodic positive solutions for a time-delayed SIR epidemic model with saturated treatment on time scales*, J. Math. Model. **9(1)** (2021) 45–60.

[20] K.V. Price, R.M. Storn, J. Lampinen, *Differential Evolution: A Practical Approach to Global Optimization*, Natural Computing Series, Springer, Berlin, 2005.

[21] D. Prodanov, *Analytical parameter estimation of the SIR epidemic model: Applications to the COVID-19 pandemic*, Entropy **23** (2021) 59.

[22] S. Rica, G.A. Ruz, *Estimating SIR model parameters from data using differential evolution: An application with COVID-19 data*, in: Proc. IEEE Conf. Comput. Intell. Bioinform. Comput. Biol. (CIBCB), 2020, pp. 1–8.

[23] M.G. Roberts, J.A.P. Heesterbeek, *A new method for estimating the effort required to control an infectious disease*, Proc. R. Soc. Lond. Ser. B Biol. Sci. **270** (2003) 1359–1364.

[24] R. Storn, K. Price, *Differential evolution — A simple and efficient heuristic for global optimization over continuous spaces*, J. Global Optim. **11** (1997) 341–359.

[25] J. Sun, X. Liu, T. Bäck, Z. Xu, *Learning adaptive differential evolution algorithm from optimization experiences by policy gradient*, IEEE Trans. Evol. Comput. **25** (2021) 1028–1041.

[26] Y. Tan, D. Cator III, M. Ndeffo-Mbah, U. Braga-Neto, *A stochastic metapopulation state-space approach to modeling and estimating COVID-19 spread*, Math. Biosci. Eng. **18** (2021) 7685–7710.

[27] R. Tanabe, A.S. Fukunaga, *Success-history based parameter adaptation for differential evolution*, in: Proc. IEEE Congr. Evol. Comput. (CEC), 2013, 71–78.

[28] G.L. Vasconcelos, A.A. Brum, F.A.G. Almeida, A.M.S. Macêdo, G.C. Duarte-Filho, R. Ospina, *Standard and anomalous waves of COVID-19: A multiple-wave growth model for epidemics*, Braz. J. Phys. **51** (2021) 1867–1883.

[29] J. Vesterstrøm, R. Thomsen, *A comparative study of differential evolution, particle swarm optimization, and evolutionary algorithms on numerical benchmark problems*, in: Proc. IEEE Congr. Evol. Comput. (CEC), Vol. 2, 2004, pp. 1980–1987.

[30] D. Wang, Y. Sun, J. Song, Y. Huang, *A SEIR model optimization using the differential evolution*, in: Lecture Notes in Comput. Sci., Vol. 12487, Springer, Cham, 2020, pp. 384–392.

[31] World Health Organization, *Pakistan COVID-19 situation reports*, WHO EMR, https://www.emro.who.int/pak/information-resources/pakistan-covid-19-situation-reports.html

[32] B. Xue, M. Zhang, W.N. Browne, *Particle swarm optimization for feature selection in classification: A multi-objective approach*, IEEE Trans. Cybern. **43** (2013) 1656–1671.

[33] I.A. Zamfirache, R.E. Precup, E.M. Petriu, *Q learning, policy iteration and actor critic reinforcement learning combined with metaheuristic algorithms in servo system control*, Facta Univ. Ser. Mech. Eng. **21** (2023) 615–630.

[34] E.K. Zavadskas, H. Dincer, S. Yuksel, S. Eti, *Intelligent expert systems using molecular fuzzy genetic algorithms and multi-objective particle swarm optimization for circular-oriented project investments*, Rom. J. Inf. Sci. Technol. **28** (2025) 260–273.

[35] W. Zhou, Z. Meng, *An adaptive differential evolution with dynamic perturbation and dimensional bidirectional crossover mechanism for diversity enhancement*, Eng. Appl. Artif. Intell. **141** (2025) 109750.